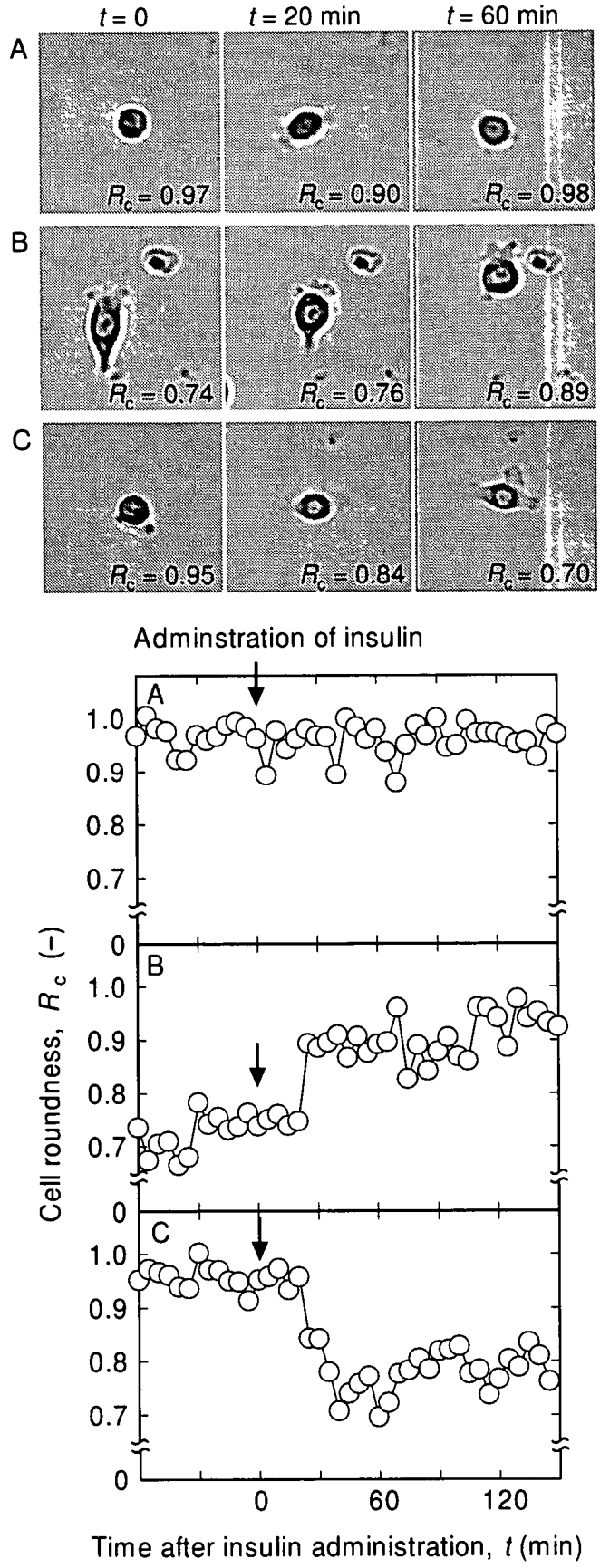


FIG. 1, Kim et al.

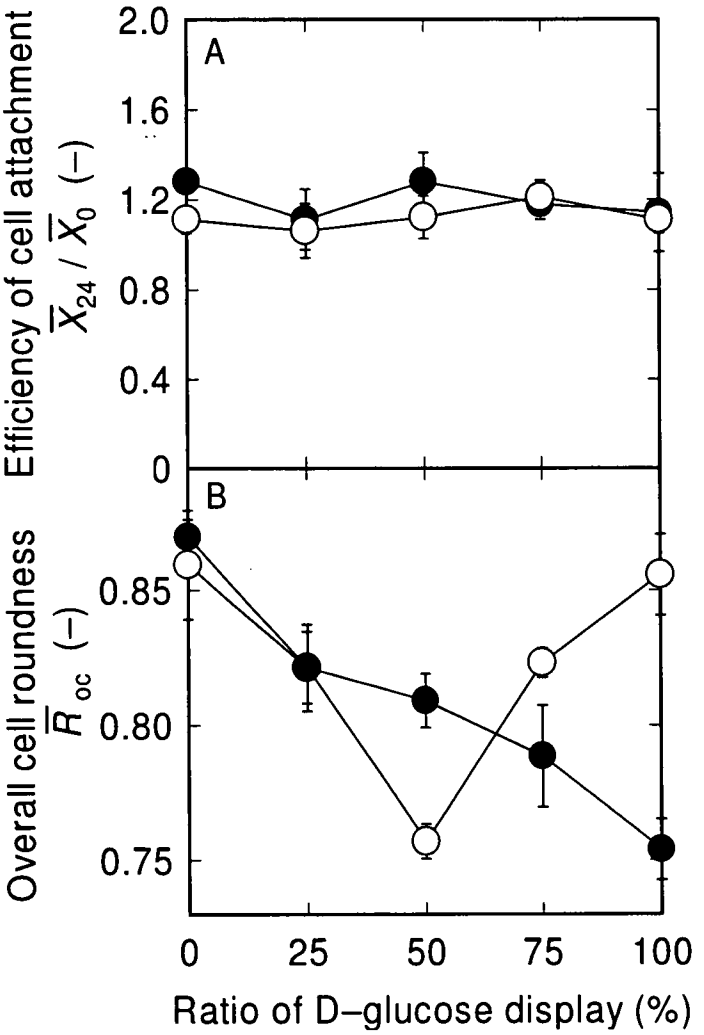


FIG. 2, Kim et al.

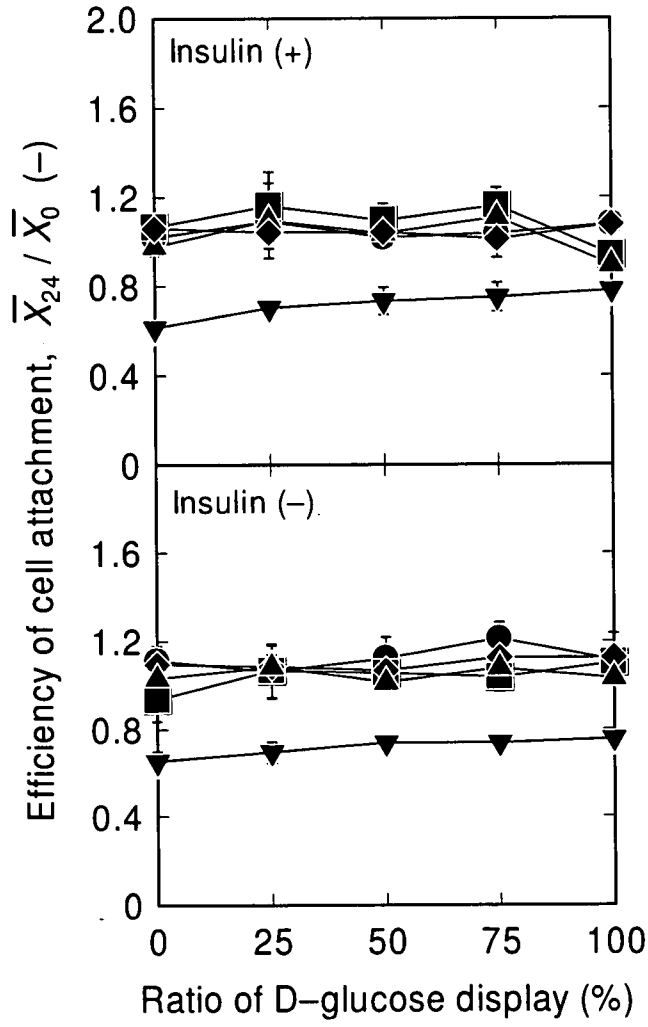


FIG. 3, Kim et al.

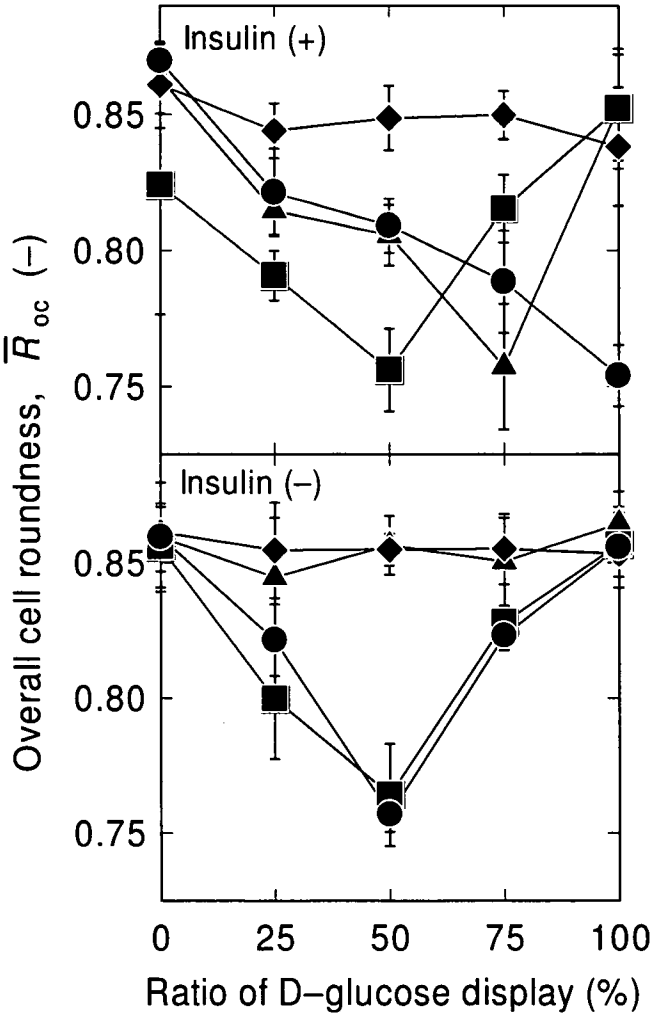


FIG. 4, Kim et al.

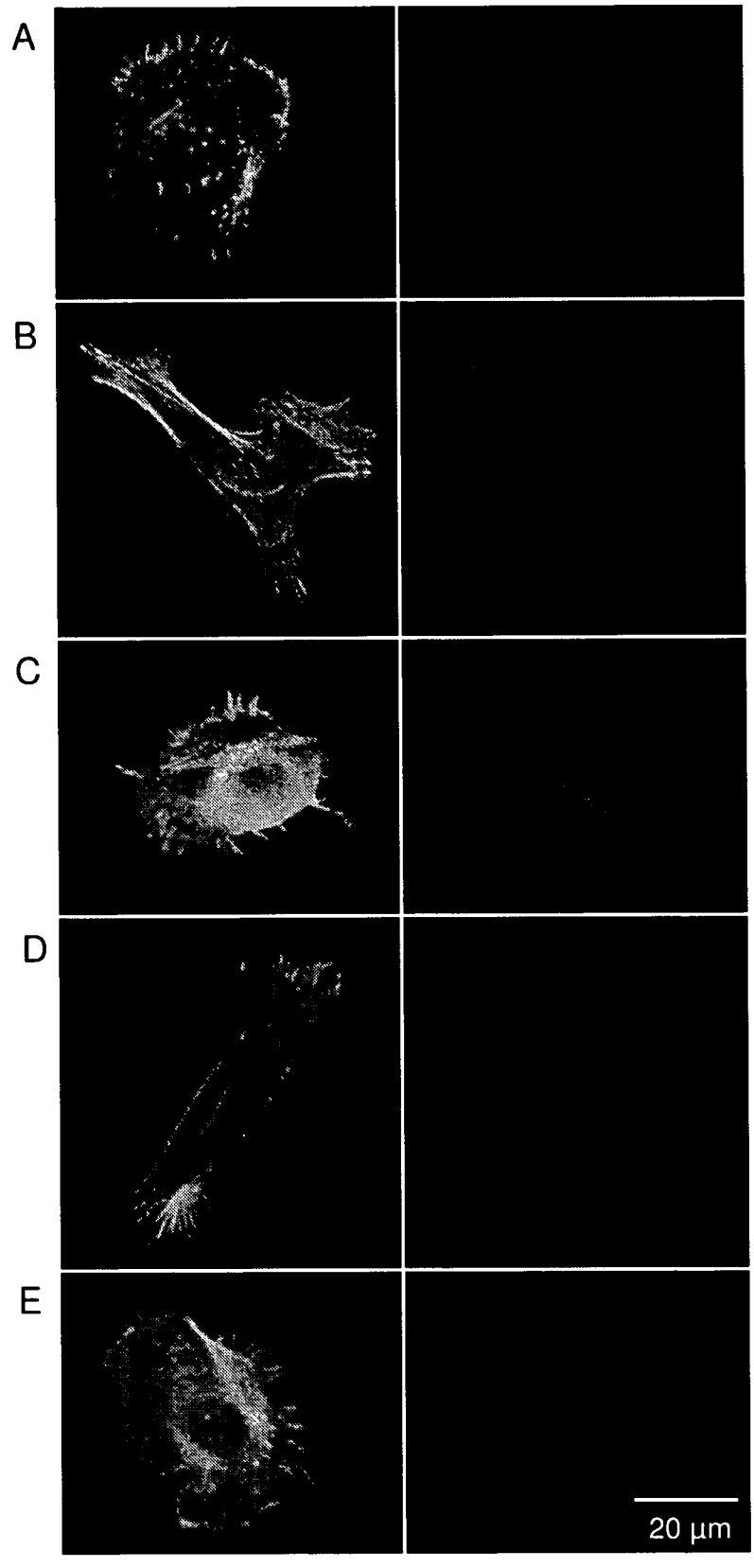


FIG. 5, Kim et al.

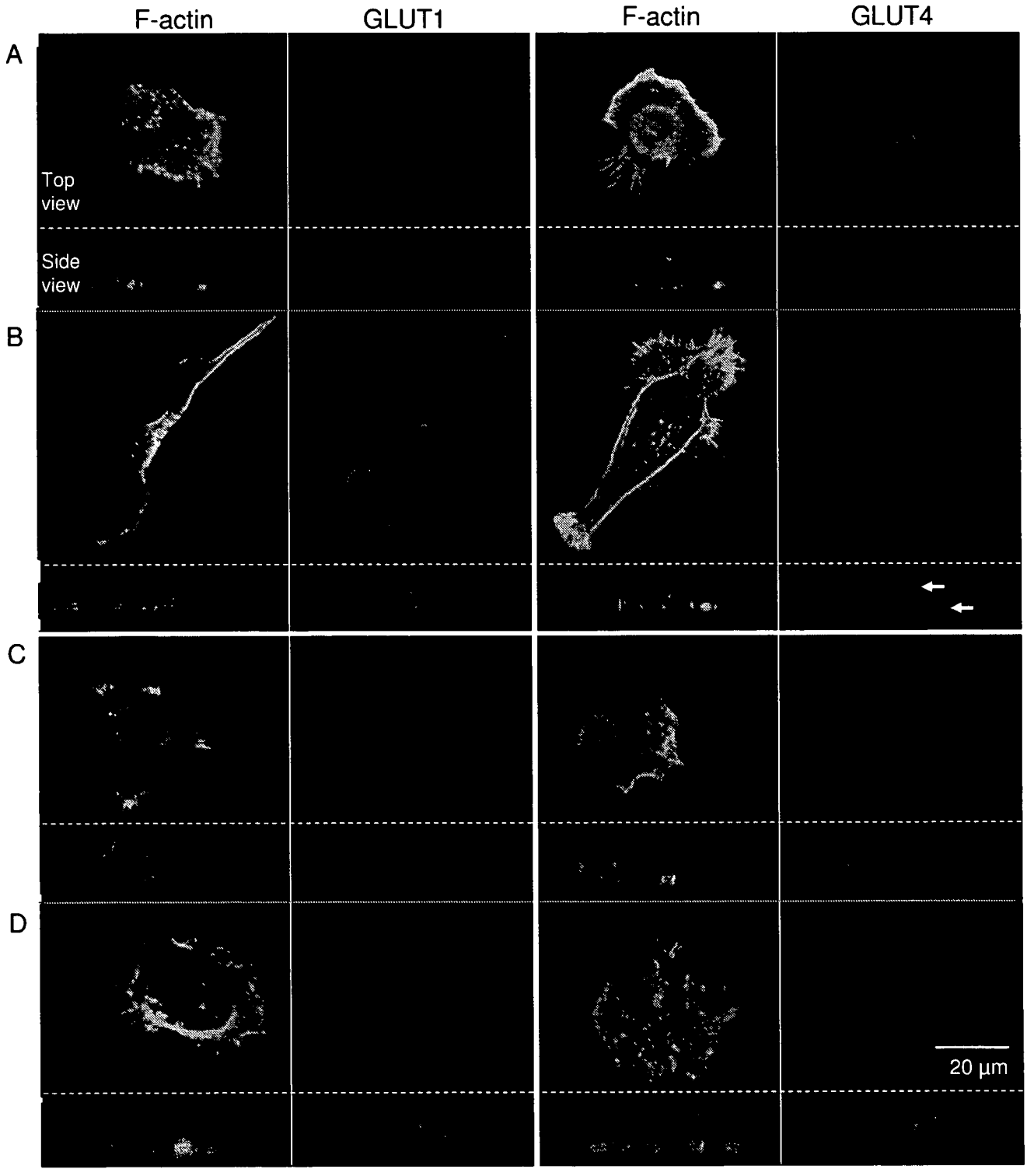


FIG. 6, Kim et al.

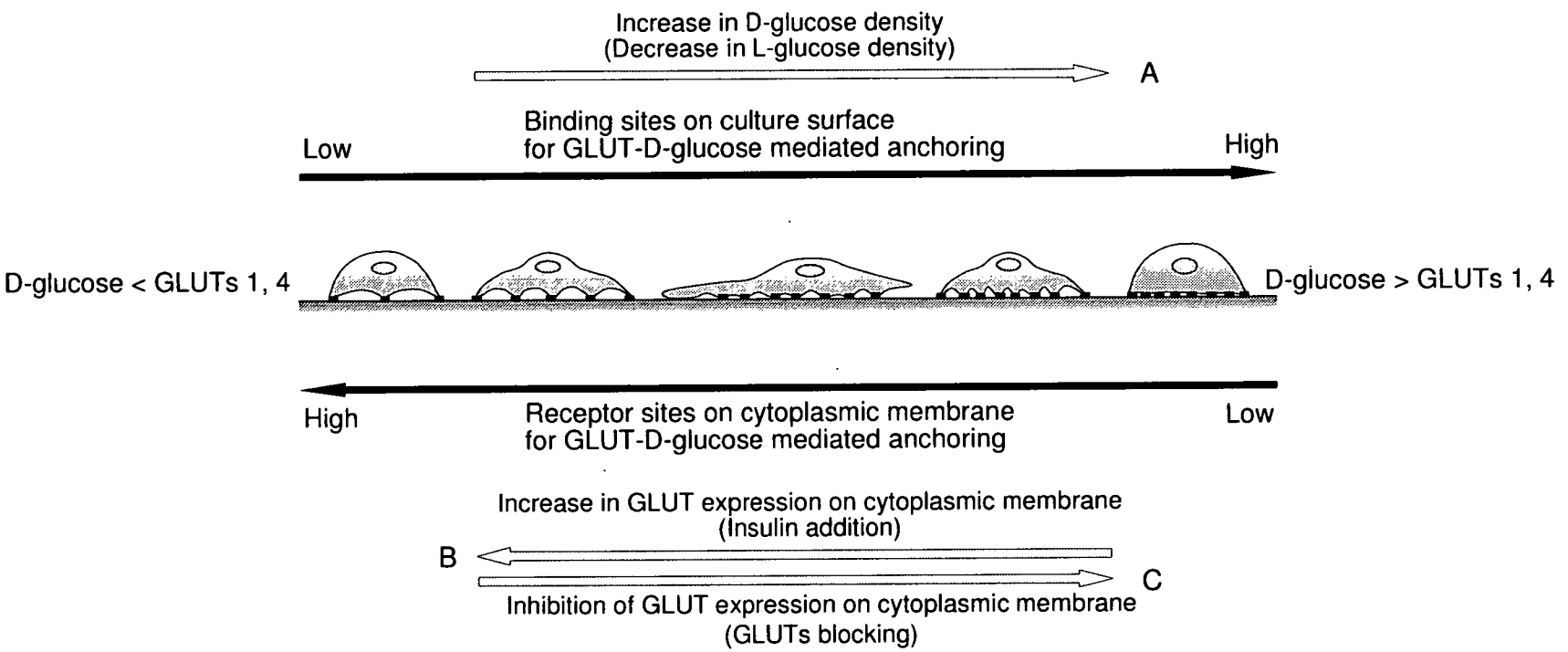


FIG. 7, Kim et al.

JOURNAL OF BIOSCIENCE AND BIOENGINEERING
Vol. 103, No. 2, 192–199. 2007
DOI: 10.1263/jbb.103.192



# Response of Human Epithelial Cells to Culture Surfaces with Varied Roughnesses Prepared by Immobilizing Dendrimers with/without D-Glucose Display

Mee-Hae Kim,[1] Masahiro Kino-oka,[2] Masaya Kawase,[3] Kiyohito Yagi,[4] and Masahito Taya[1,2]*

*Department of Biotechnology, Graduate School of Engineering, Osaka University, 2-1 Yamada-oka, Suita, Osaka 565-0871, Japan,[1] Division of Chemical Engineering, Graduate School of Engineering Science, Osaka University, 1-3 Machikaneyama-cho, Toyonaka, Osaka 560-8531, Japan,[2] Faculty of Pharmaceutical Sciences, Osaka Ohtani University, 3-11-1 Nishiki-ori, Tondabayashi, Osaka 584-8540, Japan,[3] and Graduate School of Pharmaceutical Sciences, Osaka University, 1-6 Yamada-oka, Suita, Osaka 565-0871, Japan[4]*

Received 26 September 2006/Accepted 1 December 2006

**To investigate the response of human epithelial cells to substrates with nanoscale modifications, dendrimer-immobilized surfaces were prepared with or without D-glucose displayed as a terminal ligand, giving topographic structures with mean roughnesses ($R_a$) of 1.8–11.0 nm. With an increase in the $R_a$ value up to 4.0 nm, the epithelial cells cultured on naked dendrimer surface without D-glucose display were somewhat stretched in their morphology compared with those on a nonmodified plain surface. However, for the $R_a$ values higher than 4.0 nm, such cell stretching was inhibited, resulting in the predominant existence of round-shaped cells. The change in cell morphology was appreciable on the surfaces with D-glucose-displayed dendrimers. When the $R_a$ value increased up to 4.5 nm on these surfaces, in particular, the enhancement of cell stretching was recognized, and fluorescence microscopic observation supported the hypothesis that the glucose-transporter-mediated adhesion of cells to the surface encouraged the development of filopodia and stress fibers, thereby improving focal contact with the surface. Our results suggest that the combination of displaying D-glucose and modulating roughness can promote cytoskeletal formation accompanied by marked cell elongation on culture surfaces.**

[**Key words:** human epithelial cells, dendrimer-immobilized surface, glucose display, nano-scale roughness, cell roundness, cytoskeleton, glucose transporter]

The adhesion of anchorage-dependent cells to underlying substrates modulates a variety of cellular events such as signaling, gene expression and proteogenic changes. This process involves interactions of extracellular matrix (ECM), *e.g.*, fibronectin, with the integrin family of transmembrane receptors. Integrins are major transmembrane ECM receptors and function as bidirectional transducers of signals and mechanical forces (1, 2). The integrin-mediated interactions of cells with ECM involve the formation of focal adhesion sites, which regulate signaling processes. These structurally defined adhesion sites are associated with cytoskeletal proteins by complicated mechanisms. The series of events involves the development of focal contact along with the recruitment of various cytoskeletal proteins (3, 4). The reciprocal cross-talk between these cytoskeletal systems and their adjoining substrates can give clues that can help unravel the critical regulatory pathways relating to cell morphology and motility (5, 6). Recent reports have provided new insights into these physiological interactions with respect to the process of cell adhesion to topographic surfaces (7–10). For example, it was demonstrated that the surface topography of substrates affects the cellular extension accompanied by filopodium development, indicating the existence of a favorable surface roughness on the nanoscale (11–13).

According to a review by Dalby *et al.* (13), cells encounter different topographies, ranging from macro- (tissue level) to micro- (cell level) or to nano-scales (organelle and protein levels). Microscale topographies induce changes in cell adhesion, morphology, motility and gene expression. It is most likely that these surfaces have the potential to regulate tissue organization and cell differentiation (14). On the other hand, cells are generally surrounded by nanoscale structural cues that may also be involved in controlling cell responses. Recently, manufacturing techniques for nanoscale fabrication, such as electron-beam or colloidal lithography and polymer demixing, have been made available for cell manipulations (15). Surface topography induces cellular responses to the physical architectures of substrates by affecting cell morphology, migration, proliferation and differenti-

* Corresponding author. e-mail: taya@cheng.es.osaka-u.ac.jp
phone: +81-(0)6-6850-6251 fax: +81-(0)6-6850-6254

ation (9–17).

Dendrimers are attractive owing to their chemical characteristics, because it is quite easy to modify their chemical properties by adjusting their terminal groups (18, 19). Starburst polyamidoamine (PAMAM) dendrimers are highly branched spherical polymers with well-defined structures that are soluble in aqueous solutions and have a unique surface composed of primary amino groups. PAMAM dendrimers have a core molecule, either an ammono residue as a trivalent initiator core or an ethylenediamine residue as a tetravalent initiator core, which is used to prime the stepwise polymerization, that determines several structural characteristics such as bulk, shape, density, and electrostatic charge. When an additional layer or generation is polymerized on dendrimer molecules, the number of terminal amino groups is doubled. Therefore, the defined structure and large number of terminal amino groups on dendrimers make these polymers suitable for use as biocompatible nanocapsules in gene or drug delivery systems, because of their flexibility in design variables including the ligand species present on the terminal groups as well as dendrimer size and ligand density (19–21).

In our previous studies, the potential of using dendrimers for cell processing was extended by applying this compound to a culture substratum for cell growth and differentiation. The immobilization of dendrimer was carried out to prepare the scaffold for rat hepatoma cells, and modifications of amino groups with various ligands were carried out for enhancing viability and hepatopoetic functions (22–24). In addition, a dendrimer substrate displaying D-glucose exerted a strong effect on the cellular morphology of human keratinocytes (25). In this study, various dendrimer-immobilized surfaces were prepared with different architectures by changing the generation number of dendrimers and they were characterized in terms of surface roughness by atomic force microscope (AFM). Moreover, the cellular response of human epithelial cells cultured on these surfaces was examined in terms of morphological behaviors.

## MATERIALS AND METHODS

**Surface modification** The conventional plastic culture surface of a square 8-well plate (surface area, 8.6 $cm^2$; Nunc, Roskilde, Denmark) was used as a plain or starter material. Surfaces with different topographies were obtained by immobilizing dendrimers, which were prepared through the accumulation or spherical method as illustrated in Fig. 1.

The dendrimer surfaces were designed as follows on the basis of

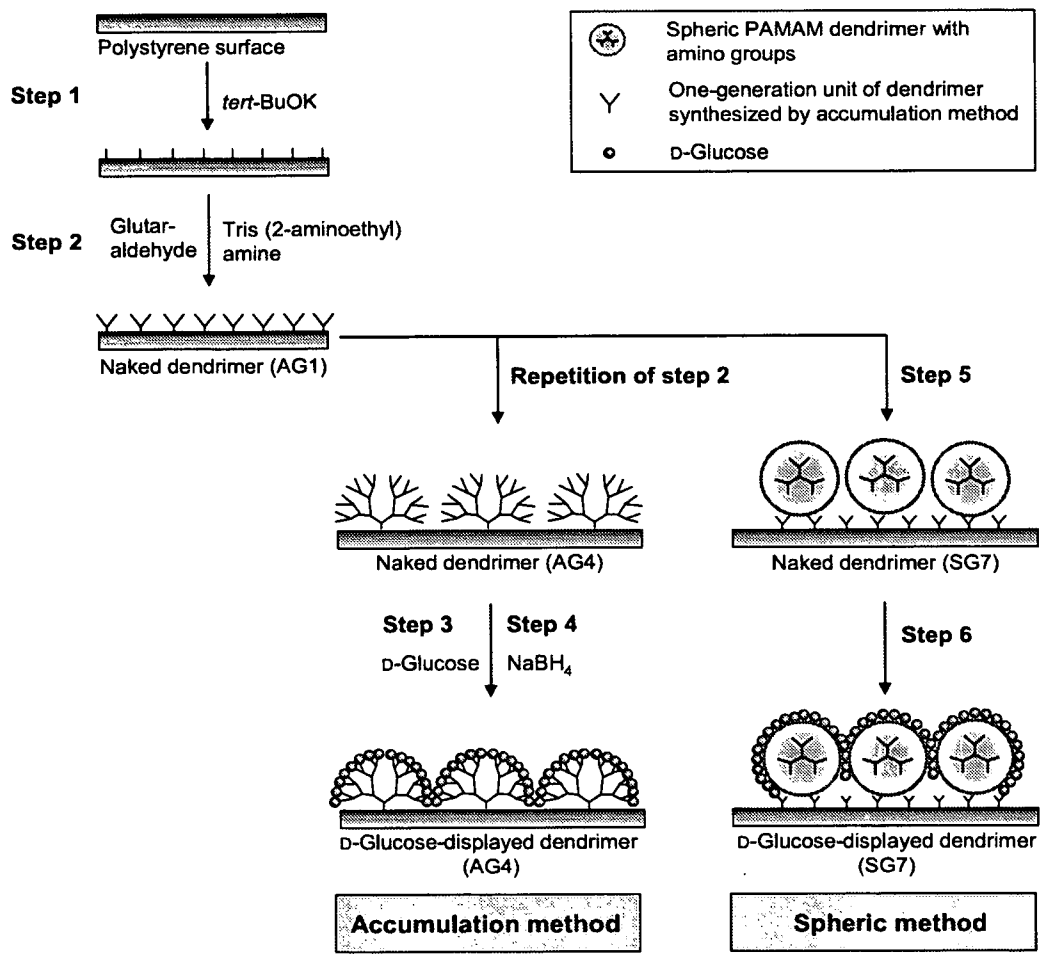


FIG. 1. Schematic illustration of processes to obtain dendrimer-immobilized surfaces with/without D-glucose display. AG and SG denote dendrimers synthesized by the accumulation and spheric methods, respectively, with the numericals showing the generation number of dendrimers.

the accumulation method. A first-generation dendrimer (denoted as AG1) was immobilized by the four-step reaction conducted under a sterile condition. Step 1: To display a hydroxyl group on the plain surface, a solution containing 50 μmol/ml potassium *tert*-butoxide (*tert*-BuOK) was poured into each well, and then the wells were incubated for 1 h at ambient temperature. The wells were then washed three times with sterilized water. The dendron core density depended on the quantity of hydroxyl groups displayed at the onset of synthesis, which can be regulated by adjusting the concentration of *tert*-BuOK. Step 2: An aqueous solution of 360 μmol/ml glutaraldehyde was introduced into the wells. The wells were allowed to stand for 1 h, followed by washing with a large amount of sterile water. The wells were then treated with 360 μmol/ml tris(2-aminoethyl) amine solution (pH 9.0, adjusted with 1 mol/dm$^3$ NaOH) for 1 h to produce a dendron structure and then rinsed with sterile water. Step 3: To display D-glucose as a terminal ligand, $0.1\times2^{n-1}$ μmol/ml D-glucose solution was added to and left to sit in the wells for 2 h ($n$: generation number). Step 4: A sodium borohydride solution (0.5 μmol/ml) was poured into the wells, and after being left to stand for 24 h, the wells were washed with sterile water, yielding the surface of first-generation dendrimer with D-glucose display. For the preparation of a culture surface with naked dendrimers (only amino group displayed), step 3 was omitted from the above-mentioned procedures.

High-generation dendrimers were prepared as follows. A solution of 360 μmol/ml glutaraldehyde was added to each well after step 2. After washing the well as described above, step 2 was conducted again. These operations were repeated until the desired generation number of dendrimers was reached. Thereafter, steps 3 and 4 were carried out for the modification of the dendrimers with D-glucose as a ligand.

The spheric method was used to prepare dendrimer surfaces with a relatively high degree of roughness. Substrates modified with spheric dendrimers at their terminal amino group were produced on the well as follows. On the first-generation dendrimer surface prepared through steps 1 and 2 by the accumulation method, spheric dendrimers were immobilized by the following reactions. Step 5: To crosslink the amino groups of spheric dendrimers, an aqueous solution of 360 μmol/ml glutaraldehyde was poured into the wells. The wells were allowed to stand for 1 h, followed by washing with a large amount of sterile water, and then a 0.05 % (v/v) aqueous solution of PAMAN spheric dendrimer (Sigma-Aldrich, St. Louis, MO, USA) was placed on the surface and left to stand for 3 h. The spheric dendrimer-immobilized surface was then rinsed with sterilized water to remove the unbound dendrimer molecules. Step 6: D-Glucose was displayed on the terminal group of immobilized dendrimers by carrying out steps 3 and 4. When necessary, the repeated steps for increasing the generation number of immobilized dendrimers, as described above, were added before step 6.

**Cell culture** A line of human mammary epithelial cells (hTERT-HME1; Clontec Laboratories, San Diego, CA, USA), which were genetically modified to have an extended cell span, was obtained as frozen cells. The cells, which were in vials, were thawed according to the supplier's manual, and then incubated in a 25-cm$^2$ T-flask (Nunclon Delta Flask; Nunc, Roskilde, Denmark). Unless otherwise stated, the cells were cultivated in serum-free medium containing 10 μg/ml insulin (HuMedia-KG2; Kurabo Industries, Osaka) at 37°C under a 5% $CO_2$ atmosphere as described elsewhere (25). For the experiments, the seeding density of viable cells, determined by trypan blue exclusion, was set at $X_0=3.0\times10^3$ cells/cm$^2$.

To estimate the concentration of adherent cells, the bottom surface image of each well was captured from three different positions using a CCD camera (CS6931; Toshiba Teli, Tokyo) attached to a microscope (area of captured image: 2.4 mm$^2$). The projected area, $A_c$, and the periphery length, $l_c$, of each cell in the cultures were determined by extracting the cellular edge on the images using a line-drawing tool on a software package (IMAQ Vision; National Instruments, Austin, TX, USA). The degree of roundness, $R_c$, of each cell was defined as follows.

$$R_c=\frac{2(\pi A_c)^{1/2}}{l_c};\ 0<R_c\leq1 \quad (1)$$

The mean value of $R_c$ was recorded as the mean of data from 50–120 cells.

**Confocal laser-scanning microscopy** The cells were subjected to F-actin and vinculin stainings as follows. The cells were fixed for 10 min at room temperature with 4% paraformaldehyde in phosphate-buffered saline (PBS), followed by being soaked in PBS with 0.1 % Triton X-100 for 4 min. The cells were then kept at 4°C for 24 h with a primary antibody against vinculin (1:400, Sigma-Aldrich) after masking nonspecific proteins for 1 h at room temperature using Block Ace (Dainippon Pharmaceutical, Osaka). The cells were washed with Tris-buffed saline (DakoCytomation Carpinteria, CA, USA), followed by immunolabeling with Alexa Fluor 594 goat anti-mouse IgG (Molecular Probes, Eugene, OR, USA) for vinculin and Alexa Fluor 488 phalloidin (Molecular Probes) for F-actin. The samples were observed under a confocal laser scanning microscope (model FV-300; Olympus, Tokyo).

**Atomic force microscopy (AFM)** An atomic force microscope (NanoScope IIIa, Digital Instruments, Santa Barbara, CA, USA) was used to characterize the topography of the prepared culture surfaces. Sample was attached to an AFM specimen disk. All the samples were analyzed in a dry state and examined in Tapping Mode with standard silicon tips (NCH-10V; Digital Instruments). The scan size of each surface was 1 × 1 μm at a rate of 1 Hz on 256 scanning lines. The analysis of topography including surface denomination was carried out using the commercially available software (SurftopEye, Mitani, Fukui). Mean roughness, $R_a$, was determined from the measurements in triplicate regions of independently prepared surfaces.

## RESULTS

**Surface design and topography** Five types of naked dendrimer surfaces, which bore an amino group as a terminal ligand, were designed by changing the generation number of dendrimers according to the preparation methods shown in Table 1. The topography of the surface was evaluated using the defined parameter of mean roughness, $R_a$. The plain surface of the well was characterized to be $R_a=0.2$ nm. With an increase in the generation number of dendrimers

TABLE 1. Mean roughnesses of prepared surfaces with dendrimers (no D-glucose display)

| Surface | | $R_a$ (nm) |
|---|---|---|
| Plain surface | | 0.2±0.0 |
| Prepared by accumulation method | AG1 | 1.8±0.2 |
| | AG2 | 2.5±0.0 |
| | AG3 | 3.5±0.6 |
| | AG4 | 4.0±0.3 |
| | AG5 | 3.6±0.1 |
| | AG6 | 4.0±0.9 |
| Prepared by spheric method | SG7 | 6.8±0.4 |
| | SG7 AG3[a] | 7.9±0.7 |
| | SG7AG5[a] | 11.0±0.6 |

[a] The spheric dendrimer was first immobilized on the surface (SG7) according to the procedure shown in Fig. 1, and then the accumulation method was applied for a further increase in the generation number of dendrimers.

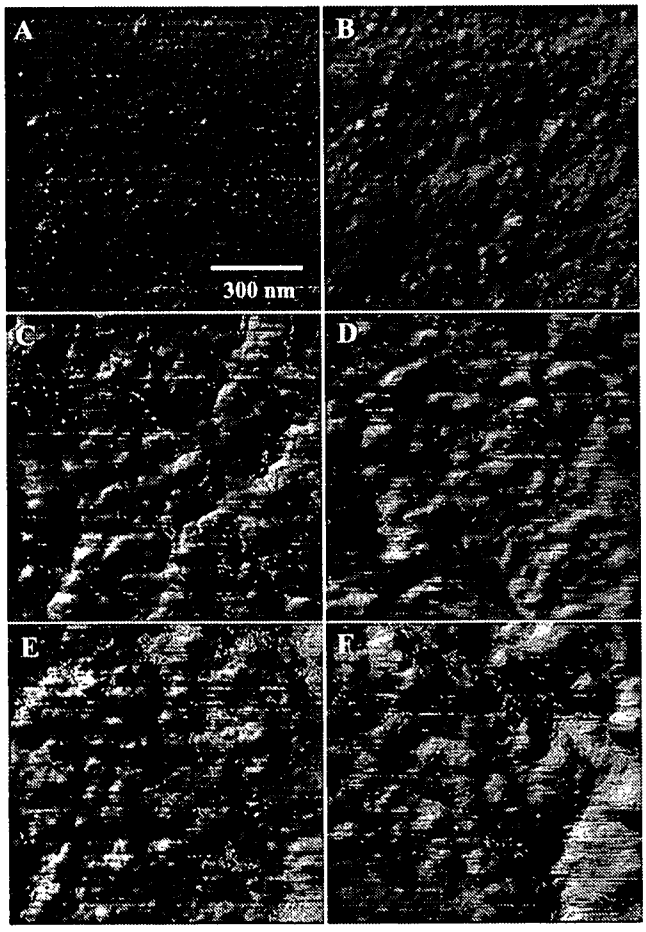


FIG. 2. Representative AFM images of naked dendrimer surfaces. (A) Plain, (B) AG1, (C) AG4, (D) AG6, (E) SG7AG3 and (F) SG7AG5 surfaces.

for the accumulation method, the $R_a$ value increased, giving $R_a$=4.0 nm for the 4th-generation dendrimer surface (denoted as AG4). On the contrary, the value of $R_a$ did not increase for the naked dendrimer surface of the 5th or 6th generation (3.6 nm for AG5 and 4.9 nm for AG6).

The spherical dendrimer was thought to produce a higher degree of roughness on the surface owing to its structure. In this study, spherical dendrimers of the 7th generation, which possessed a theoretical diameter of 8.1 nm (19), were immobilized as a framework of the convex surface. The $R_a$ value of this surface (denoted as SG7 in Table 1) reached 6.8 nm, and further development caused an increase in the $R_a$ value, yielding $R_a$=11.0 nm for the SG7AG5 surface, which had the highest $R_a$ value of the dendrimer surfaces prepared in this study. Figure 2 shows the architectures of the selected surfaces. According to the $R_a$ value, indented topographies were observed on the respective dendrimer surfaces; in contrast, the plain surface exhibited a relative smoothness. For the D-glucose-displayed dendrimer surfaces prepared, similar topographies were recognized, and their $R_a$ values were slightly higher than those of the naked dendrimer surfaces (data not shown). Thus, variation in the generation numbers and preparation methods can endow surfaces with different nanoscale topographies.

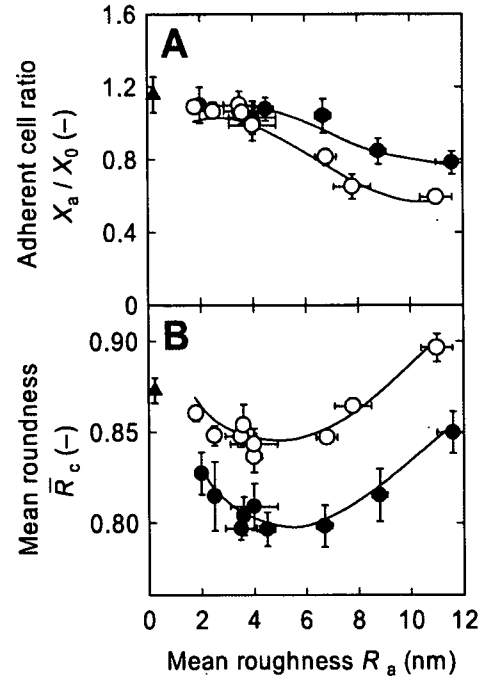


FIG. 3. Effects of mean roughness on attachment and morphology of human epithelial cells cultured on various dendrimer-immobilized surfaces. Plots of (A) $X_a/X_0$ and (B) $\bar{R}_c$ against $R_a$, determined at 24 h of culture time. Error bars indicate standard deviations ($n$=3). Symbols: closed circles, D-glucose-displayed dendrimer surface; open circles, naked dendrimer surface; and closed triangles, plain surface.

**Attachment of cells to designed surfaces** To investigate cellular responses to the naked and D-glucose-displayed dendrimer surfaces, the cultures of human epithelial cells were conducted, and 24 h after seeding, the ratio of adherent cells to seeded cells, $X_a/X_0$, was determined. As shown in Fig. 3A, with an increase in the $R_a$ value of the naked dendrimer surface, the value of $X_a/X_0$ decreased ($X_a/X_0$=0.6 when $R_a$=11.0 nm), while the $X_a/X_0$ value on the plain surface was 1.2. The $X_a/X_0$ values of the D-glucose-displayed dendrimer surfaces also decreased with an increase in the $R_a$ value, although the level of $X_a/X_0$ was slightly higher than that of the naked dendrimer surface with larger value of $R_a$. These results suggest that roughness can inhibit cellular access to the surface and that the display of D-glucose suppress such inhibition to some extent.

**Cellular morphology on designed surfaces** To investigate the interaction between the cells and surfaces, cellular morphology was observed 24 h after seeding. With an increase in the $R_a$ value up to 4.0 nm, the cells on the naked dendrimer surface were somewhat stretched. The cellular morphology was quantified in terms of the mean degree of cell roundness, $\bar{R}_c$. As shown in Fig. 3B, on the naked dendrimer surfaces with the $R_a$ values up to 4.0 nm, a slight decrease in $\bar{R}_c$ value was found compared with the $\bar{R}_c$ value of the plain surface. A further increase in the $R_a$ value, however, caused less cell extension with an increase in $\bar{R}_c$ value, and round-shaped cells prevailed with $\bar{R}_c$=0.9 at $R_a$=11.0 nm. For D-glucose-displayed dendrimer surfaces, the morphological change with the $R_a$ value showed a similar tendency to that of the naked dendrimer surface, although the increase

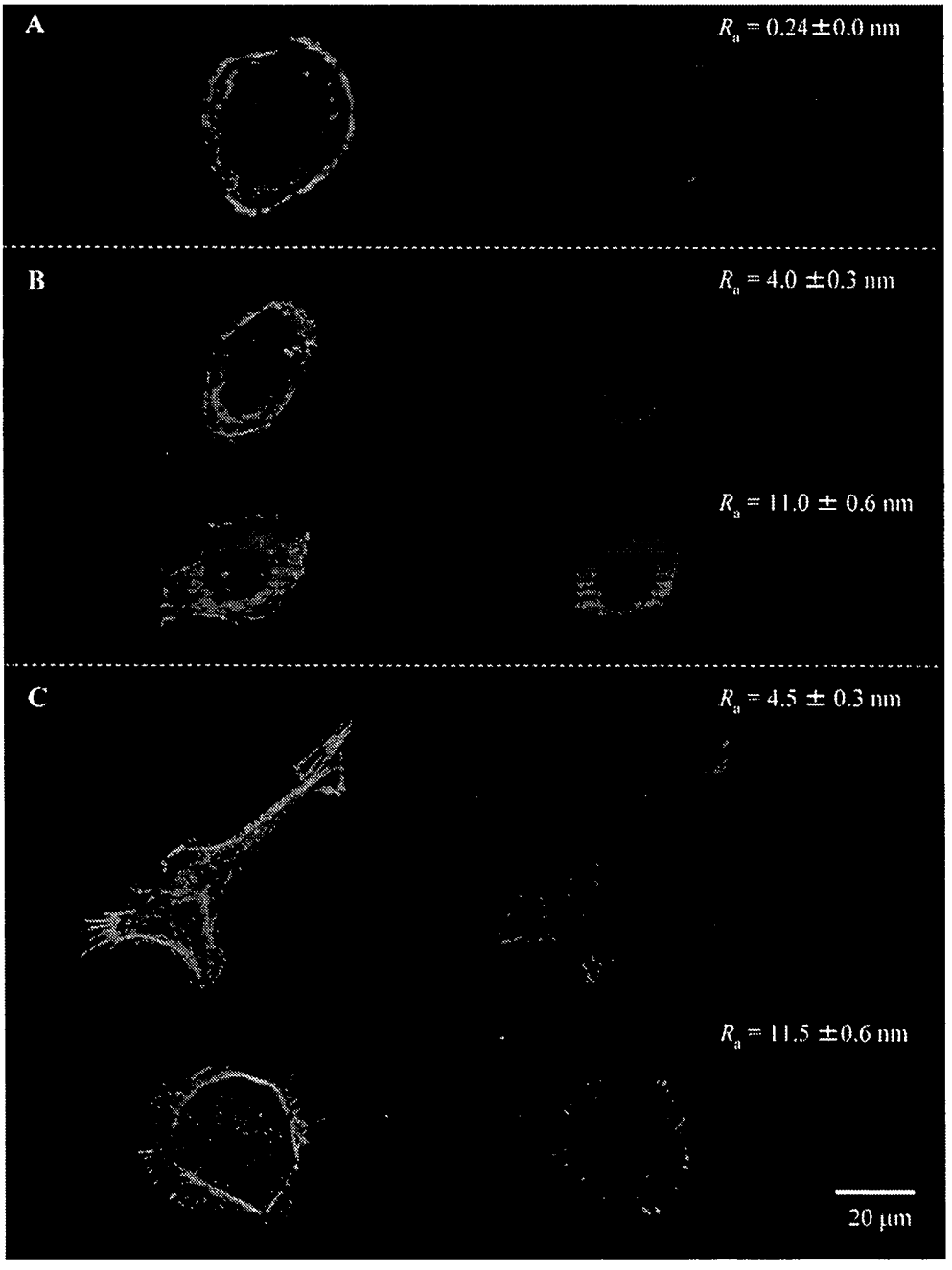


FIG. 4. Immunostaining of actin cytoskeleton (green) and vinculin (red) of human epithelial cells cultured for 24 h on dendrimer-immobilized surfaces with various values of mean roughness. (A) Plain, (B) naked dendrimer and (C) D-glucose-displayed dendrimer surfaces.

in the population of stretched-shape cells was significant, resulting in the lower values of $\bar{R}_c$ in the entire range of $R_a$ values examined. On the D-glucose-displayed dendrimer surface at $R_a$=6.7 nm, the value of $\bar{R}_c$ was minimized to 0.8, which is much smaller than the minimal $\bar{R}_c$ value of the naked dendrimer surface at $R_a$=4.0 nm. Thus, the cell morphology was remarkably altered as a result of the roughness of the culture surface.

To clarify the cytoskeletal organization and focal contact with the dendrimer surface, the cells were observed 24 h after seeding by the fluorescence stainings of F-actin and vinculin. As seen in Fig. 4B, the epithelial cells cultured on the naked dendrimer surface with $R_a$=4.0 nm were abundant in F-actin filaments of peripheral stress fibers and filopodia, compared with those cultured on the plain surface (Fig. 4A). However, the cells on the naked dendrimer surface with $R_a$=11.0 nm showed a poor organization of stress fibers with punctuate actin as well as less developed filopodia (Fig. 4C). For the cells on the D-glucose-displayed dendrimer surfaces with $R_a$=4.5 nm, on the other hand, fully organized actin stress fibers with distinct vinculin spots appeared in both the cytoplasm and the cell periphery, whereas nebular vinculin was only observed in the cell periphery on the corresponding naked dendrimer surfaces (Fig. 4B). For the

cells on the D-glucose-displayed dendrimer surface with $R_a$=11.5 nm, the stress fibers in cytoplasm disappeared. Thus, the cell staining analyses revealed that surface roughness affects the formation of F-actin filaments which are used to organize filopodia and stress fibers. In addition, the D-glucose display enhanced the development of stress fibers with distinct spots of vinculin. These findings support the hypothesis that the grasping of the glucose transporter in the cytomembrane with D-glucose immobilized on the surface facilitates the frequent formation of cell-surface contact.

## DISCUSSION

Culture surface is a kind of reaction field in which anchorage-dependent cells show behaviors of attachment, migration and division. Many researchers have paid their attention to gene transfer and the stimulation of receptors on the plasma membrane through interactions with solid surfaces. The interactive effectiveness of biologically active components can be improved by arraying them in close contact with targets on the cell membrane, because the dispersed components in bulk liquid (medium) are less able to approach the targets. The methodological development of component display on culture surfaces is considered to be one of the most critical issues. Dendrimers have recently become of interest as synthetic chemicals that provide a promising template for an effective gene delivery system obtained by changing the generation number of dendrimers and ligand species. When dendrimers are deposited on a solid surface, their unique properties are expected to yield physical and chemical variations in surface roughness, dendrimer density, and ligand species attached to and their amounts on the dendrimers, together with the locality of displayed ligands. In the present study we focused on the influences of roughness and ligand type on the cellular response by changing the generation number of dendrimers with or without D-glucose display.

Surface roughness governs cell morphology, which depends on cytoskeletal formation involving the development of actin stress fibers and dynamic links with filopodia. Dalby *et al.* (13) reported that the development of F-actin filaments is promoted in fibroblasts on a surface modified with a moderate roughness, even though excess roughness inhibited such development, being poor in attachment of round-shaped cells compared with that on a nonmodified plain surface. This trend was concordant with our results obtained in the cultures of epithelial cells on the dendrimer surfaces with various mean values of roughness. Filopodium development in the cells on the naked AG4 dendrimer surface ($R_a$=4.0 nm) was promoted compared with that in the cells on the plain surface. However, a further increase in degree of roughness suppressed its development, and the cells cultured on the naked SG7AG5 dendrimer surface ($R_a$=11.0 nm) exhibited punctuate and nebulous actins (see Fig. 4).

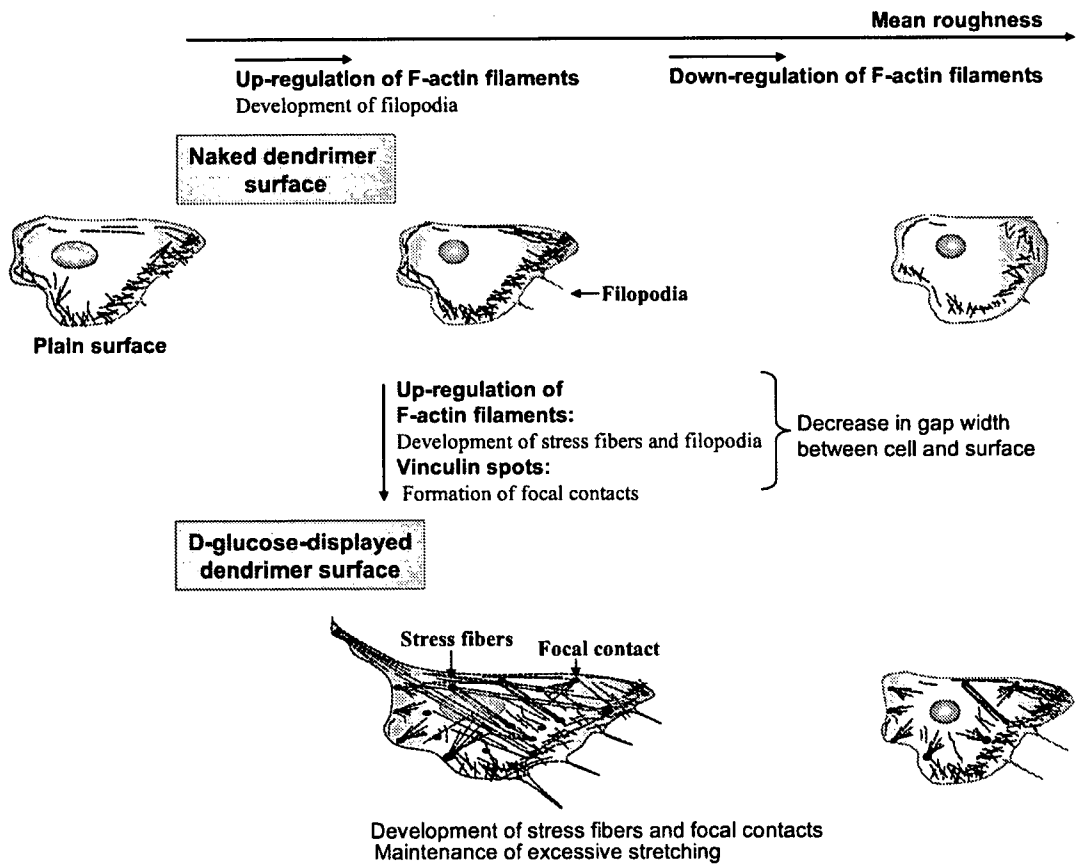


FIG. 5. Conceptual illustration showing morphological changes of human epithelial cells cultured on various dendrimer-immobilized surfaces with/without D-glucose display.

Surfaces with the functional groups of biologically active molecules have been designed for targeting integrins and their receptors on cellular membrane (26, 27). Current researches have been focused on developing surfaces modified with physicochemically well-defined, biomimetic materials that have various properties such as a low protein-adsorbing, for dealing with the control of cytomembrane-mediated interactions to promote cellular functions (28–30).

The uptake of D-glucose from medium is mediated through the glucose transporters (GLUTs), which essentially have no affinity for its optical isomer L-glucose on the plasma membrane of cells. Therefore, D-glucose display on surfaces enable its binding to ventral GLUTs on the membrane, which permits the cells to anchor partially by temporally grasping GLUTs. In addition, cell migration relates dynamically to the assembly of filopodium actin filaments appearing at the leading edge and the disassembly of such filaments at the tail, which are responsible for the extension and retraction of cells, respectively. The partial anchoring through GLUTs seems to prevent retraction in the rear of cells based on the consideration that the suppression of filament disassembly causes excessive cellular elongation. This idea supports the view that GLUTs may make a certain contribution to the cellular elongation observed in this study. With regard to dynamic links and cytoskeleton formation, D-glucose display on the surface induced clearly defined actin filaments of filopodia and stress fibers, respectively (see Fig. 4). In addition, the vinculin spots at the terminals of stress fibers indicated mature focal contacts, unlike for the naked dendrimer surface, on which the cells exhibited a smaller number of actin filaments with nebular vinculin expression. The changes in cell shape as well as the potentials of anchorage and motility are mainly associated with a dynamic reorganization of the filament arrays that make up the actin cytoskeleton. The activation of individual members of the Rho family (small G proteins) modulates the organization of actin filaments in cells, with Rho activation resulting in the formation of stress fibers with focal contacts, which are involved in the formations of Rac-inducing lamellipodia and Cdc42-inducing filopodia (4).

Figure 5 illustrate a possible mechanism of the morphological response of epithelial cells to the dendrimer-immobilized surfaces with or without D-glucose display. It is proposed that D-glucose displayed on dendrimers permits the cells to be in close contact with the surface through the grasping of GLUTs on the plasma membrane, being attributable to the up-regulation of focal contact formation. In addition, this GLUT-mediated grasping promoted the development of stress fibers in the cytoplasm particularly at moderate mean roughnesses of approximately 4.5 nm, resulting in the excessively stretched shape of cells. Therefore, surface roughness and D-glucose display induce changes in cellular morphology caused by alternation in the cytoskeleton in response to focal contact formation. In conclusion, in this study, we propose that dendrimer surfaces will offer a promising design for human epithelial cell stimulators by the surface-localized display of suitable ligands targeting receptors on cell membrane.

## ACKNOWLEDGMENTS

This study was conducted as part of the programs "Center for integrated cell and tissue regulation" for the Center of Excellent (21st COE) and "Multidisciplinary research laboratory system" organized in the Graduate School of Engineering Science, Osaka University. This study also received financial support in part by a Grant-in-Aid for Scientific Research (no. 17360398) from the Ministry of Education, Culture, Sports, Science and Technology and by a grant for Research on Human Genome, Tissue Engineering and Food Biotechnology from the Ministry of Health, Labour, and Welfare, Japan.

## REFERENCES

1. **Martin, K. H., Slack, J. K., Boerner, S. A., Martin, C. C., and Parsons, J. T.:** Integrin connections map: to infinity and beyond. Science, **296**, 1652–1653 (2002).
2. **Gumbiner, B. M.:** Cell adhesion: the molecular basis of tissue architecture and morphogenesis. Cell, **84**, 345–357 (1996).
3. **Geiger, B., Bershadsky, A., Pankov, R., and Yamada, K. M.:** Transmembrane crosstalk between the extracellular matrix-cytoskeleton crosstalk. Nat. Rev. Mol. Cell Biol., **2**, 793–805 (2001).
4. **Sastry, S. K. and Burridge, K.:** Focal adhesions: a nexus for intracellular signaling and cytoskeletal dynamics. Exp. Cell Res., **261**, 25–36 (2000).
5. **Bernhard, W. H. and Beat, A. I.:** Actin, microtubules and focal adhesion dynamics during cell migration. Int. J. Biochem. Cell Biol., **35**, 39–50 (2003).
6. **Schwartz, M. A. and Ginsberg, M. H.:** Networks and crosstalk: integrin signalling spreads. Nat. Cell Biol., **4**, 65–68 (2002).
7. **Curtis, A. and Wilkinson, C.:** Topographical control of cells. Biomaterials, **18**, 1573–1583 (1997).
8. **Frey, M. T., Tsai, I. Y., Russell, T. P., Hanks, S. K., and Wang, Y.-I.:** Cellular response to substrate topography: role of myosin II and focal adhesion kinase. Biophys. J., **90**, 3774–3782 (2006).
9. **Mustafa, K., Odén, A., Wennerberg, A., Hultenby, K., and Arvidson, K.:** The influence of surface topography of ceramic abutments on the attachment and proliferation of human oral fibrablasts. Biomaterials, **26**, 373–381 (2005).
10. **Ponsonnet, L., Comte, V., Othmane, A., Lagneau, C., Charbonnier, M., Lissac, M., and Jaffrezic, N.:** Effect of surface topography and chemistry on adhesion, orientation and growth of fibroblasts on nickel-titanium substrates. Mater. Sci. Eng. C, **21**, 157–165 (2002).
11. **Hatano, K., Inoue, H., Kojo, T., Matsunaga, T., Tsujisawa, T., Uchiyama, C., and Uchida, Y.:** Effect of surface roughness on proliferation and alkaline phosphatase expression of rat calvarial cells cultured on polystyrene. Bone, **25**, 439–445 (1999).
12. **Fan, Y. W., Cui, F. Z., Hou, S. P., Xu, Q. Y., Chen, L. N., and Lee, I.-S.:** Culture of neural cells on silicon wafers with nano-scale surface topography. J. Neurosci. Methods, **120**, 17–23 (2002).
13. **Dalby, M. J.:** Topographically induced direct cell mechanotransduction. Med. Eng. Phys., **27**, 730–742 (2005).
14. **Curran, J. M., Chen, R., and Hunt, J. A.:** The guidance of human mesenchymal stem cell differentiation *in vitro* by controlled modifications to the cell substrate. Biomaterials, **27**, 4783–4793 (2006).
15. **Yim, E. K. and Leong, K. W.:** Significance of synthetic nanostructures in dictating cellular response. Nanomedicine, **1**, 10–21 (2005).
16. **Diehl, K. A., Foley, J. D., Nealey, P. F., and Murphy, C. J.:** Nanoscale topography modulates corneal epithelial cell mi-

gration. J. Biomed. Mater. Res., **75A**, 603–611 (2005).
17. **Loesberg, W. A., Walboomers, X. F., van Loon, J. J. W. A., and Jansen, S. A.:** The effect of combined hypergravity and microgrooved surface topography on the behaviour of fibroblast. Cell Motil. Cytoskeleton, **63**, 384–394 (2006).
18. **Lee, C. C., Mackay, J. A., Fréchet, J. M. J., and Szoka, F. C.:** Designing dendrimers for biological applications. Nat. Biotechnol., **23**, 1517–1526 (2005).
19. **Tomalia, D. A., Huang, B., Swanson, D. R., Brothers, H. M., and Klimash, J. W.:** Structure control within poly (amidoamine) dendrimers: size, shape and region-chemical mimicry of globular proteins. Tetrahedron, **59**, 3799–3813 (2003).
20. **Bielinska, A., Kukowska-Latallo, J. F., Johnson, J., Tomalia, D. A., and Baker, J. R., Jr.:** Regulation of *in vitro* gene expression using antisense oligonucleotides or antisense expression plasmids transfected using starburst PAMAM dendrimers. Nucleic Acids Res., **24**, 2176–2182 (1996).
21. **Lai, J. C., Yuan, C., and Thomas, J. L.:** Single-cell measurements of polyamidoamine dendrimer binding. Ann. Biomed. Eng., **30**, 409–416 (2002).
22. **Kawase, M., Kurikawa, N., Higashiyama, S., Miura, N., Shiomi, T., Ozawa, C., Mizoguchi, T., and Yagi, K.:** Immobilization of ligand-modified polyamidoamine dendrimer for cultivation of hepatoma cells. Artif. Org., **24**, 18–22 (2000).
23. **Kawase, M., Kurikawa, N., Higashiyama, S., Miura, N., Shiomi, T., Ozawa, C., Mizoguchi, T., and Yagi, K.:** Effectiveness of polyamidoamine dendrimers modified with tripeptide growth factor, glycyl-L-histidyl-L-lysine, for enhancement of function of hepatoma cells. J. Biosci. Bioeng., **88**, 433–437 (1999).
24. **Higashiyama, S., Noda, M., Kawase, M., and Yagi, K.:** Mixed-ligand modification of polyamidoamine dendrimers to develop an effective scaffold for maintenance of hepatocyte spheroids. J. Biomed. Mater. Res., **64A**, 475–482 (2003).
25. **Hata, N., Kim, M.-H., Isoda, K., Kino-oka, M., Kawase, M., Yagi, K., and Taya, M.:** Dendrimer-immobilized culture surface as a tool to evaluate formation of cellular cytoskeleton of anchorage-dependent cells. J. Biosci. Bioeng., **97**, 222–238 (2004).
26. **Gilbert, M., Giachelli, C. M., and Styton, P. S.:** Biomimetic peptides that engage specific integrin-dependent signaling pathways and bind to calcium phosphate surfaces. J. Biomed. Mater. Res., **67A**, 69–77 (2003).
27. **García, A. J.:** Get a grip: integrins in cell-biomaterial interactions. Biomaterials, **26**, 7525–7529 (2005).
28. **Hersel, U., Dahmen, C., and Kessler, H.:** RGD modified polymers: biomaterials for stimulated cell adhesion and beyond. Biomaterials, **24**, 4385–4415 (2003).
29. **García, A. J. and Reyes, C. D.:** Engineering integrin-specific surfaces with a triple-helical collagen-mimetic peptide. J. Biomed. Mater. Res., **65A**, 511–523 (2003).
30. **Lieb, E., Hacker, M., Tessmar, J., Kunz-Schughart, L. A., Fiedler, J., Dahmen, C., Hersel, U., Kessler, H., Schulz, M. B., and Göpferich, A.:** Mediating specific cell adhesion to low-adhesive diblock copolymers by instant modification with cyclic RGD peptides. Biomaterilas, **26**, 2333–2341 (2005).

年4回発行(2005年12月発行)

ISSN1344-1221

NPO日本医工学治療学会 機関誌

Winter 2005

# 医工学治療

Therapeutics & Engineering

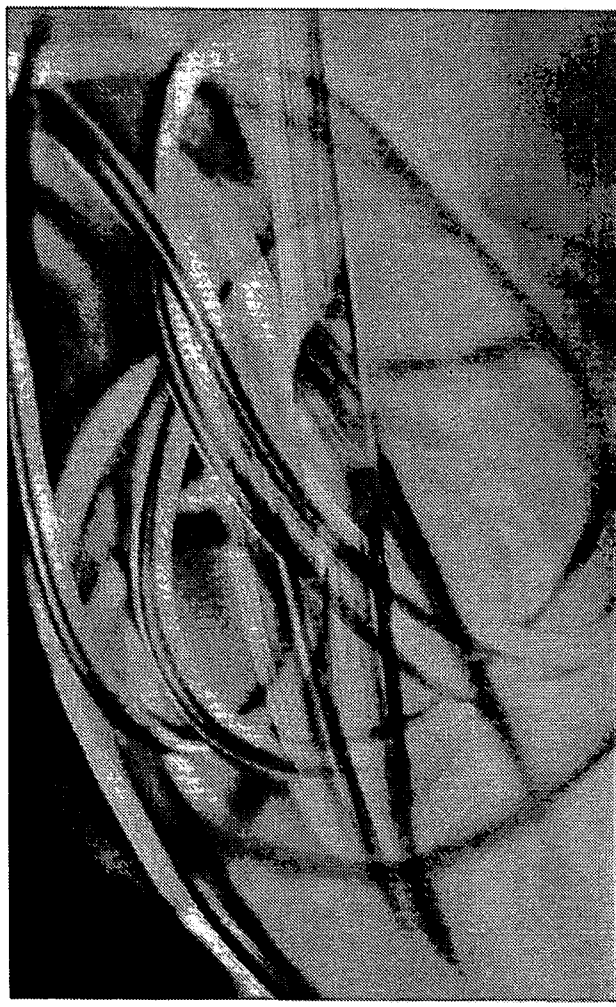

特集 生物化学工学からの再生医療への取り組み 酒井康行



vol.17 no.4

通巻50号

特定非営利活動法人日本医工学治療学会

Japanese Society for Therapeutics & Engineering

NPO 日本医工学治療学会　機関誌
# 医工学治療
Therapeutics & Engineering
vol. 17 NO.4
2005. 12

CONTENTS

# 移植を前提とした組織培養工程における細胞評価

大阪大学大学院 基礎工学研究科

紀ノ岡 正博　田谷 正仁

## 1．はじめに

組織工学における基礎および実践研究において、細胞増殖および分化のための培養環境を調整（細胞、足場、シグナル伝達因子の調和）する培養技術と*in vitro*で組織の再構築を行った後、患者の患部に移植する再生医療技術が開発されてきた。組織工学製品の産業化のためには、これらの研究を橋渡しする工学的な展開研究も重要とされているが、培養工学的観点からみると、現状の培養組織作製は、洞察力に長けた熟練オペレータの手作業によるもので、産業規模での生産には不向きとなっている[1,2]。培養組織の品質を評価するための細胞診断は、一般的には、襲撃的、破壊的な手法に依存しているが、培養組織の生産工程においては、評価のために原料である細胞を消費することは、生産原理および原料の希少性から避ける必要がある。よって、培養中、細胞接触することなく検査を行うか、一時的な検査の後再び原料としての使用を可能とするような、細胞を再利用できる細胞診断システムが不可欠である。また、多くの培養は、比較的少量（100cm$^3$まで）で行われ、複数ラインでの培養が要求されるため、いわば少量多品種での生産様式がとられる。その結果、培養容器としては、小型、単純でかつディスポーサブルなものが多い。しかし、いかなる単純な容器での培養においても、細胞を取り巻く環境を厳密に制御しつつモニタリングを行うことが必要となり、非襲撃かつ非破壊のセンシングツールの開発が望まれている。本稿では、細胞挙動を観察する上での装置構築およびデータ解析の考え方、実際の培養操作から得られる情報を利用した細胞診断技術について紹介する。

## 2．組織工学製品の生産における細胞診断[3]

単層増殖時においては、培養容器底面からの細胞観察は、迅速かつ簡易で最も有効な培養状況の把握手段である[1-3]。細胞観察手法は、大きく2つに分けられる。**図1**に示すように、静止画（snapshot）のようにある特定の時間において観察する方法（end-point observation）は、簡易かつ安価で一般的な顕微鏡などの装置で行うことができる（静的評価、static evaluation）。その結果、汎用性が高く、多くの研究や生産の現場で、日々熟練オペレータが、細胞形態を顕微鏡下で観察し、培養環境の状況把握に努めている。しかし、容器内全体での細胞形態の集団的観察となるため、化学反応とのアナロジーの観点で考えると、いわゆる平衡論的な情報のみが取得可能である[6]。一方、培養面への接着を伴う足場依存性細胞において、細胞運動は培養環境を把握する上で重要な評価要素である。個々の細胞の動画（movie）のような経時的観察（time-lapse observation）は、より高質な情報が得られ、速度論的な解析を行うことができるが、装置、操作が煩雑になり汎用性に乏しい（動的評価、dynamic evaluation）[5,7-10]。

培養中の細胞挙動を実際に観察するにあたって、**図2**に示すように、培養系の不均質性および不均一性を考慮し

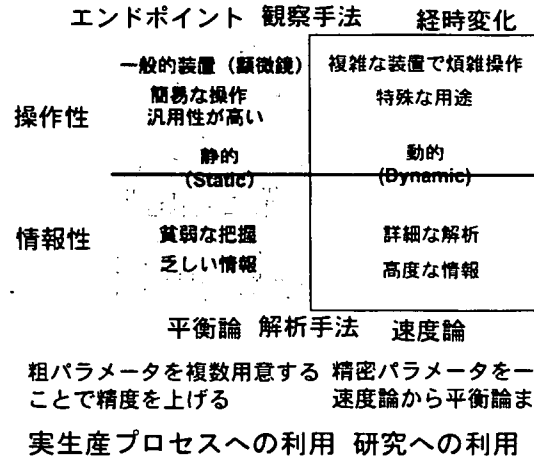


図1　細胞観察手法

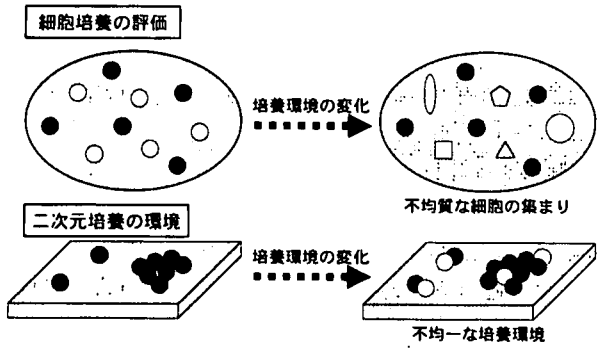


図2　細胞培養における不均質，不均一性について

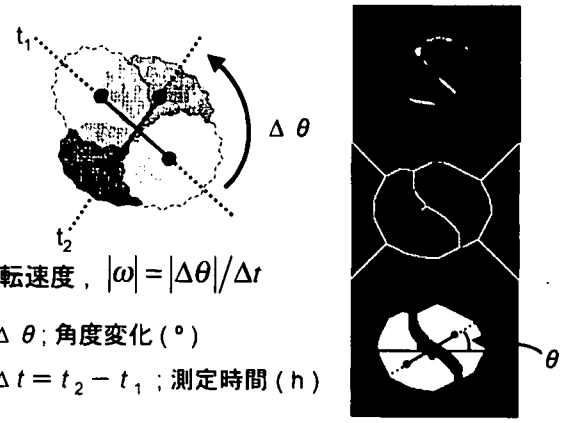


図4　細胞ペアーの回転運動に対する数値化

た情報取得が必要となる。均一に見える細胞でも、培養経過による環境の変化によって個々の細胞で挙動が異なり、不均一な細胞集団となる。足場依存性細胞の単層増殖では、細胞が培養面に接着し細胞分裂を繰り返すため、単独状態もあれば、集団状態もあり細胞の配置状態によって、その培養環境は不均一なものとなる。従来の物質生産などを目的としたセルライン（株化細胞）を用いた細胞培養における評価では、**図3**に示すように、集団細胞を均質として捉え、かつ培養環境も均一状態であると考え、刺激などの変数に対し、単方向へ応答（"均質応答"）する。その結果、その一部の細胞を観察し培養全体の代表値として、平均値比較（有意差判定）や単純相関評価を行ってきた。しかし、組織培養のために採取された細胞（新鮮細胞）では、増殖や分化、細胞年齢などの複数

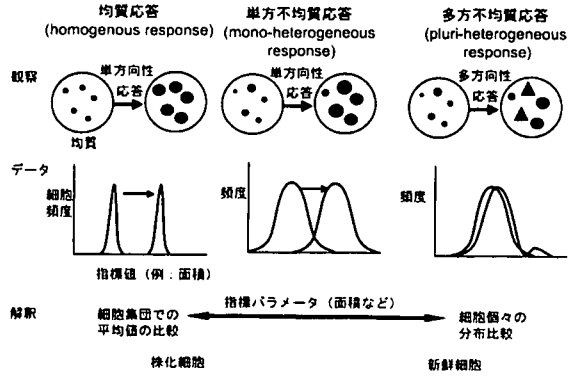


図3　不均質を考慮したデータ取得方法

の現象が絡み合って生じる。よって、単方向性応答でも不均質な応答（"単方不均質応答"）を示し、分散の大きな平均値比較で解釈することとなる。さらに、分化の方向性が複数存在する場合には、多方向を示す応答（"多方不均質応答"）であると考えられ、個々の単方不均質応答の統合の結果、平均値比較（有意差判定）や単純相関評価ではデータの差異を見出すことが困難で、データ処理の工夫が必要となる。一般には、多方不均質応答に対し、蛍光試薬による染色（標的化）にて有用データを絞って（情報抽出）から解析を行うことで、よりデータの精度を高めている。無染色での細胞評価でも、標的化、情報抽出は不可欠で、従来の有意差判定や単純相関評価のみならず、多重相関評価、抽出挙動評価、on-off評価などの処方により精度向上を目指す。これらの手法は、精度や操作性の点で特徴があり、用途に応じた選択が必要である。以下には、一例として、動的かつ抽出挙動評価について紹介する。

## 3．細胞運動の観察[5) 9)]

個々の細胞の挙動観察は細胞内外の状態を把握する上で重要な情報を与えうる。フラスコ内で多点観察が可能な細胞観察装置にて、ヒト上皮細胞の挙動観察（動的評価）を行ったところ、1個の細胞の並進運動はほとんどみられないが、2個の細胞が接した状態になると回転運動を行うことがわかった。そこで、**図4**に示すように、個々の

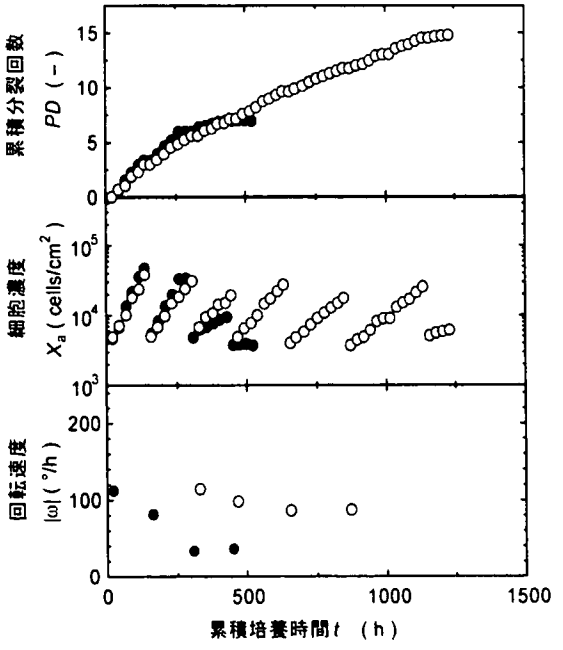


**図5　角化細胞の継代培養における細胞濃度変化と運動能力の経過**
**(●：通常酸素濃度条件下、○：極低酸素濃度条件下)**

重心間を結ぶ直線の傾きを算出する画像解析プログラムを構築し、重心間の直線が$\Delta t$時間に回転する角度$\Delta\theta$より、2個の細胞の回転速度（$|\omega|=|\Delta\theta|/\Delta t$）を評価した（抽出挙動評価）。さらに、培養環境を変化させ運動性を示す本指標の変化を検討したところ、細胞内ATP濃度と関連性が存在し、細胞増殖能と運動能力の相関を得ることができた。

回転速度による細胞挙動評価の有効性を確認するため、通常酸素濃度（21%）と極低酸素濃度（0.2%以下）の条件下における角化細胞の継代培養実験を実施した。**図5**に示すように、通常酸素濃度下で培養した場合は、数回の継代培養において累積分裂回数$PD=6.8$で細胞の増殖が停止し寿命に達するのに対し、極低酸素濃度では増殖速度の著しい低下もなく増殖が続いた。その結果$PD=14.5$となり、通常酸素濃度下で培養したときの約2.1倍となった。さらに、各酸素濃度下で培養したときの細胞挙動を把握するために、回転速度を測定した。通常酸素濃度下では累積分裂回数の増加とともに、回転速度が低下したが、極低酸素濃度下での培養では、寿命に伴う回転速度の著しい低下は見られなかった。累積分裂回数が増加しても細胞内ATP量に差は見られなかったことから、寿命が遅延してもATPが生成され、回転速度は低下せず、細胞活性が維持されていると考えられる。

以上の結果より、低酸素濃度では寿命に伴う細胞活性の低下が抑制されるだけでなく、累積分裂回数が増加し、寿命が遅延され、角化細胞からなる表皮シート生産プロセスに対して、有効な培養操作となりうることがわかった。また、回転速度を指標とする運動性評価は、細胞活性評価の一つとして有効であることが示された。さらに、回転運動能力と細胞伸展能力の組み合わせ評価により、角化細胞の継代培養中に、細胞寿命を非侵襲的に評価可能であることを確認した[10]。

## 4. おわりに

培養組織生産における非侵襲的細胞観察は、本稿で示したように、ほとんどが単層状態、つまり、継代培養においてのみ実施可能で、三次元構造を持つ組織培養には適用が困難である。しかし、継代培養において、多くの観察情報を取得・解析し，培養シミュレーター（仮想培養）との組み合わせで、生産工程全般における時間的予測や培養組織内の空間的予測を可能とし、将来的には、継代培養中の細胞評価が、製品評価につながるものと考えられる。今後は、細胞評価や培養シミュレータの技術を駆使することで、製品評価のための規格化が必要となるであろう。

謝辞：本研究の概念構築は、大阪大学大学院基礎工学研究科 未来研究ラボシステムおよび厚生労働科学研究費補助金の支援を受けて行っております。

(http://www.sigma.es.osaka-u.ac.jp/pub/mrl/).

**文献**

1) 紀ノ岡正博，田谷正仁：ものづくりから見た再生医療—培養組織の生産—．バイオサイエンスとバイオインダストリー 61